

Phenomenological Effects and Container Pressurization during Thermal Decomposition of Polyurethane Foams

**A. B. Dodd, K. L. Erickson, E. C. Quintana, and
R. E. Hogan Jr.**

**Sandia National Laboratories
Albuquerque, New Mexico, USA**

VNIIA-SNL Technical Exchange

6-9 August 2012

**Sandia is a multi program laboratory operated by Sandia Corporation, a Lockheed Martin Company,
for the United States Department of Energy's National Nuclear Security Administration
under contract DE-AC04-94AL85000.**



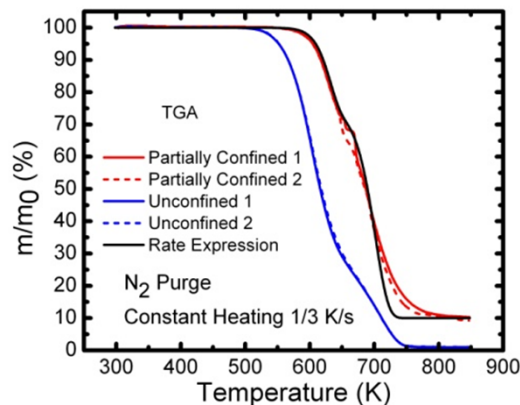
Polymer foams provide thermal, mechanical, & electrical isolation in engineered systems

- Systems safety analyses use numerical models to predict heat transfer to encapsulated objects and pressurization/failure of sealed containers
- In inert environments, the incident heat flux to a system can cause foams to decompose
- Evolved gases can cause pressurization and failure of sealed containers
- Container pressurization involves complex physics
 - Liquefaction/flow introduces convective heat transfer
 - Erosive channeling by hot gases exacerbates liquefaction/flow
 - Pressure depends on rate of gas generation, which depends on temperature history (Heat transfer through foam is more important)

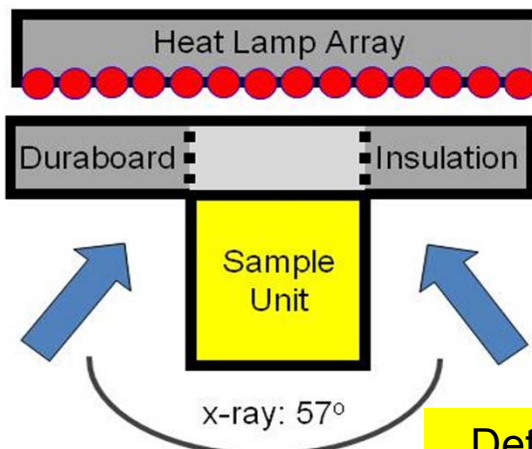


Coordinated experiments & analyses are needed to develop models for systems safety analyses

Material properties from independent laboratory experiments



Small container heat transfer and pressurization experiments



3

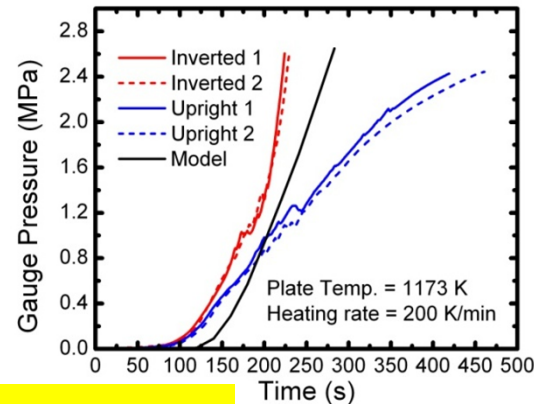
Develop model based on existing radiation-conduction code

$$\rho c \frac{\partial T}{\partial t} = \nabla \bullet (k + k_e) \nabla T + \sum_i \rho r_i (-\Delta H_i)$$

$$P = n_g R / \int_{V_g} \left(1/T \right) dV_g$$

Reaction rate expressions for r_i & n_g

Evaluate models: compare with results from container experiments



Determine needed experiments and model/code development

Small container heat transfer & pressurization exp's. provide physical insight and T & P data

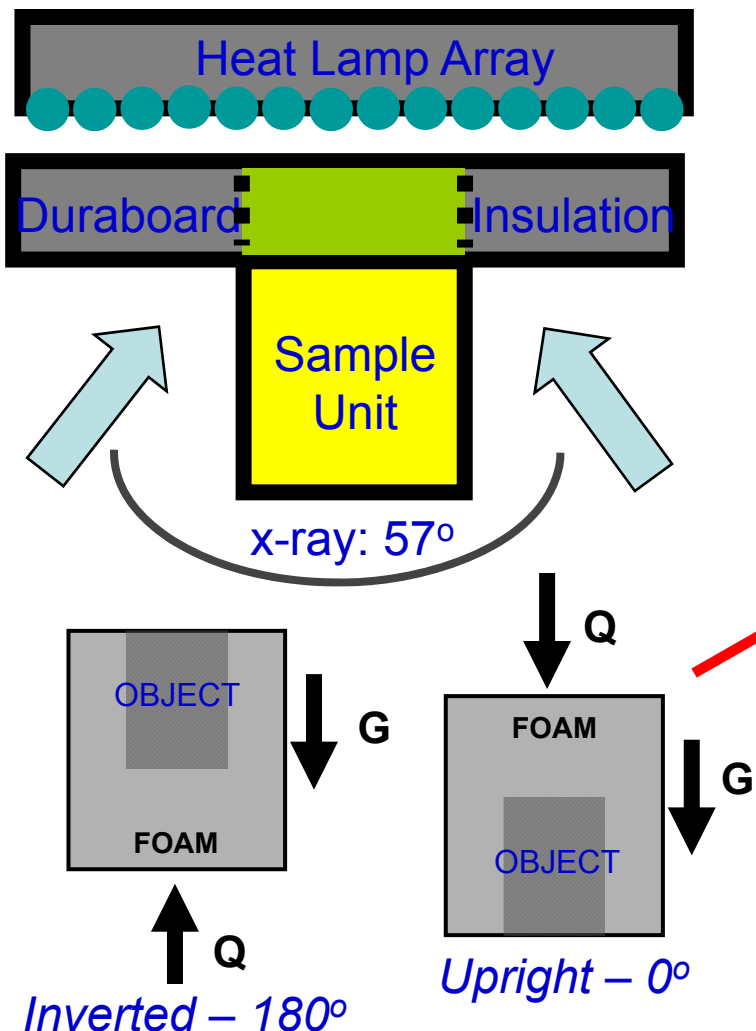
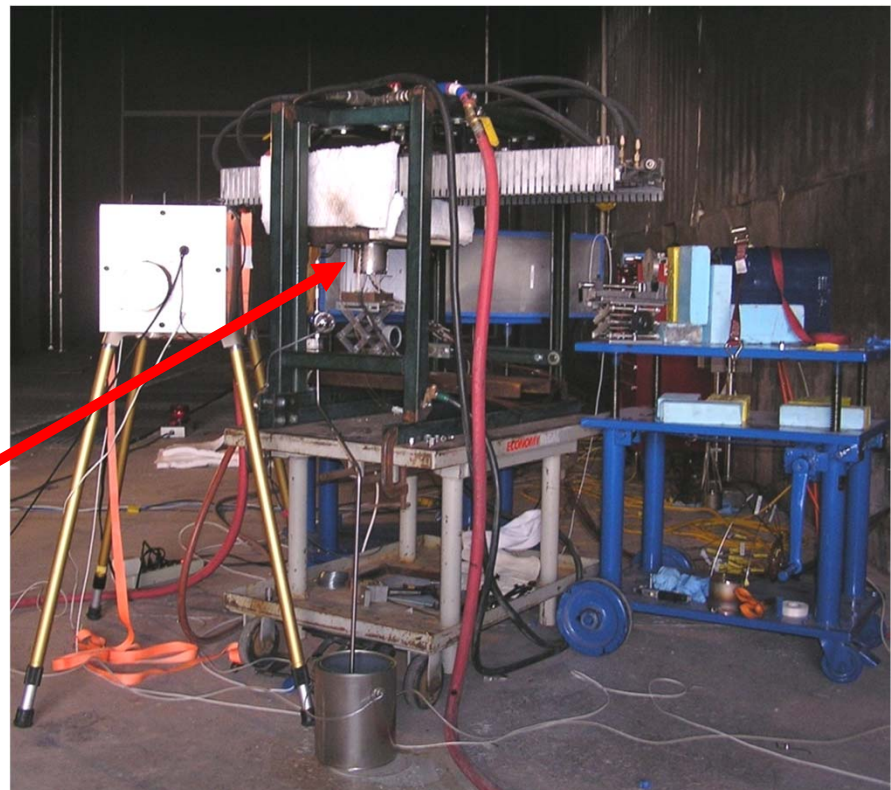
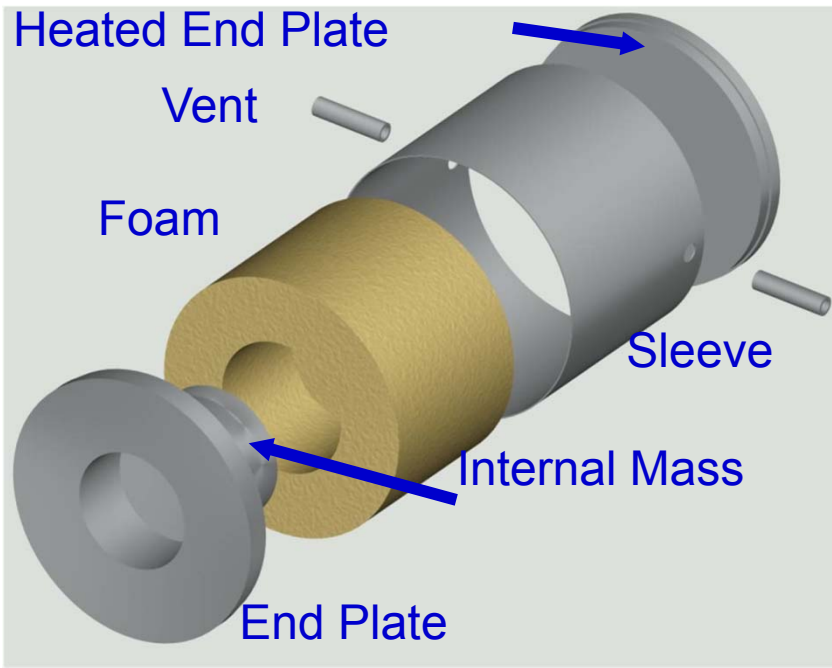


Plate temperature: 1173 K
Foam density = 160 to 720 kg/m³

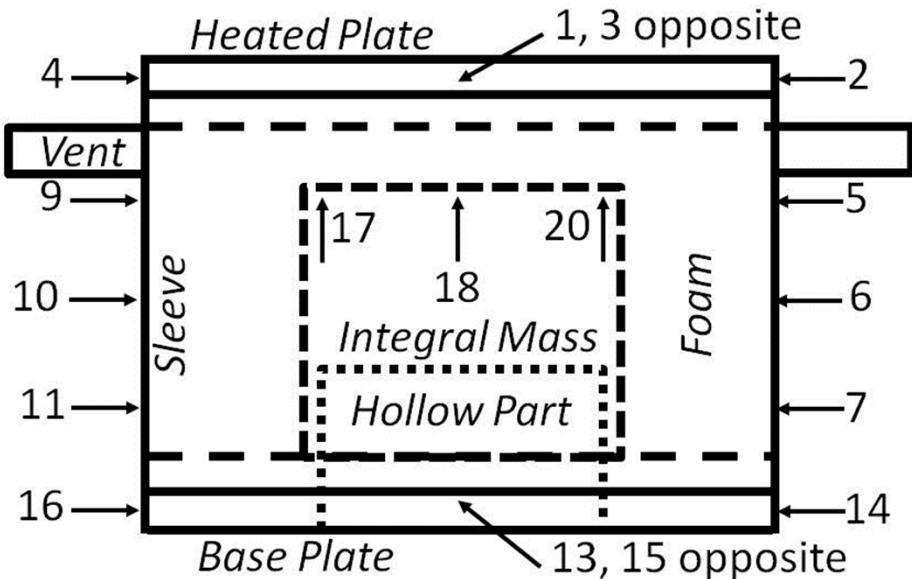


Experiments were done using *foam-in-can* (FIC) configuration



Sample container

- Sleeve 321 SS tubing
 - 8.89-cm OD, 5.40 cm long
 - 0.508-mm wall thickness
- End plates: 0.475-cm thick 304 SS
 - Laser welded to Sleeve



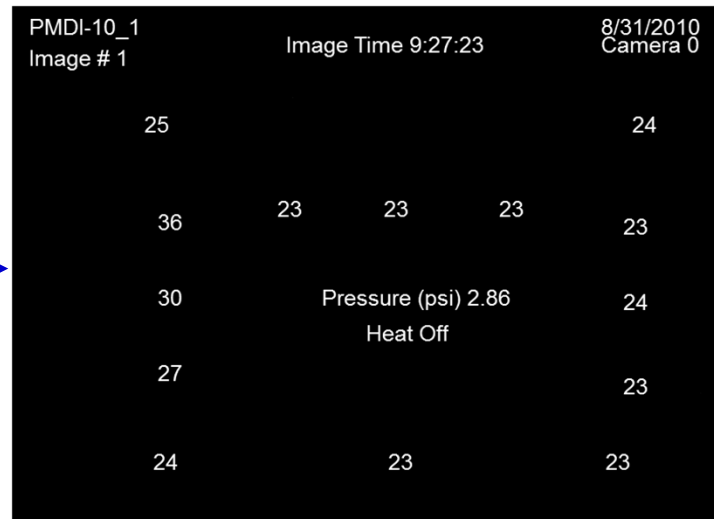
Rigid, closed cell, polyurethane foams

- TDI-polyester-polyol
 - (160 - 720 kg/m³)
- PMDI-polyether-polyol
 - 160 & 320 kg/m³

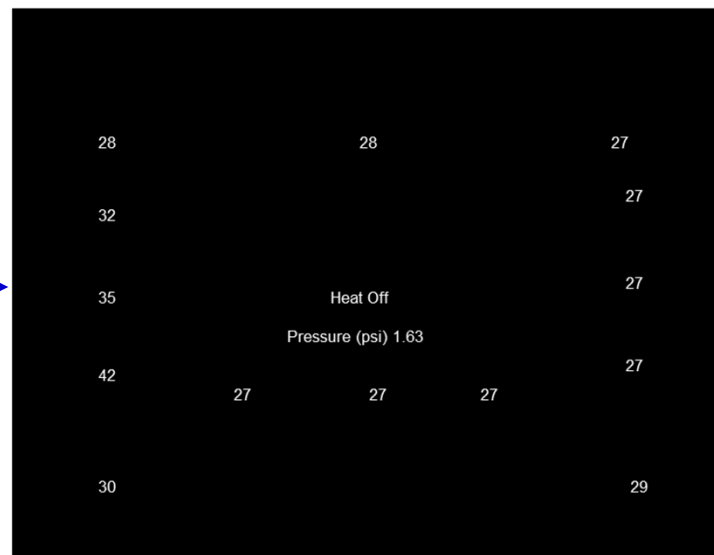
X-ray images showed liquefaction and flow occurring with lower density PMDI-based polyurethane foam

PMDI-based foam
160 kg/m³

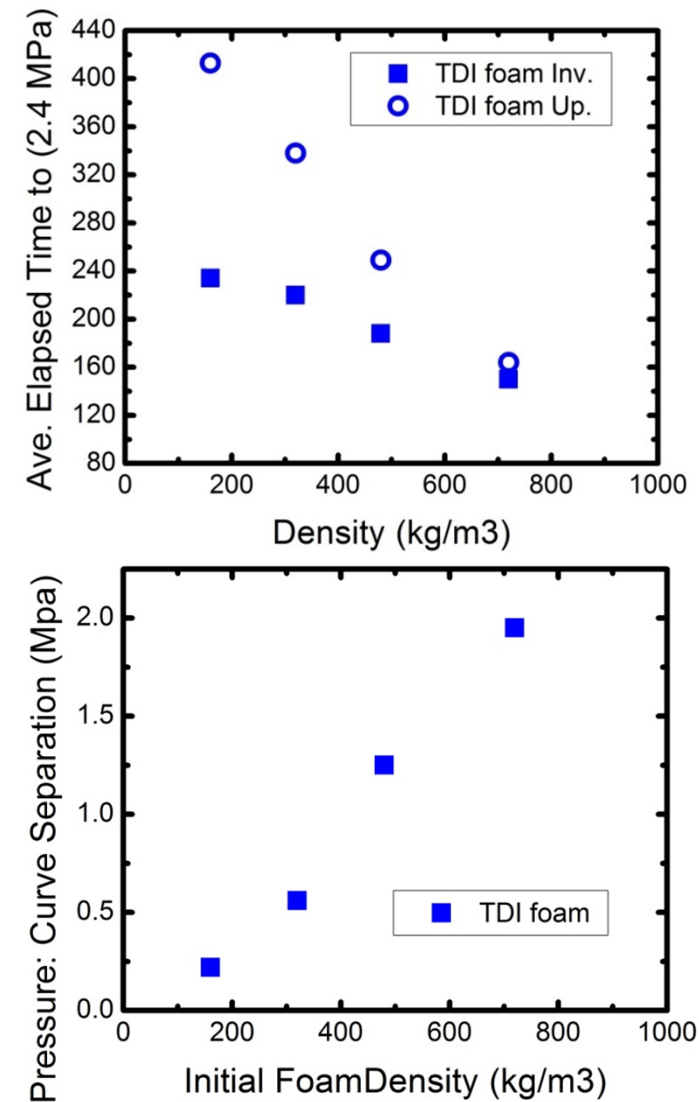
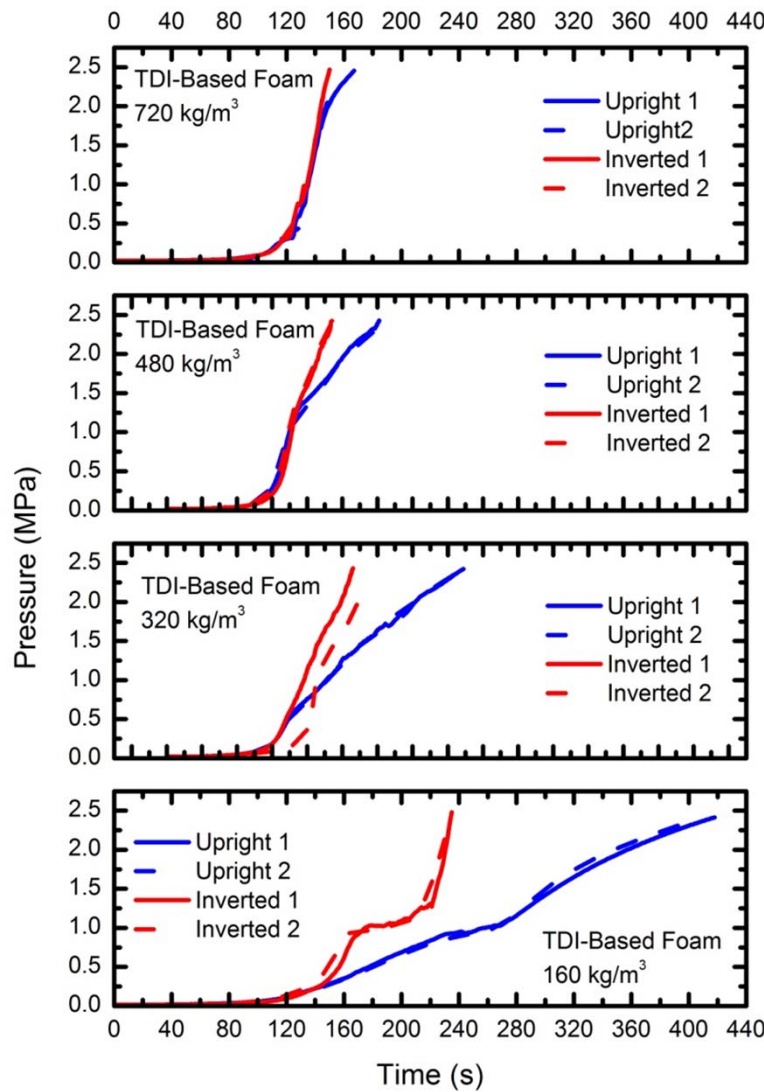
Bulk movement
was away from →
the heat source



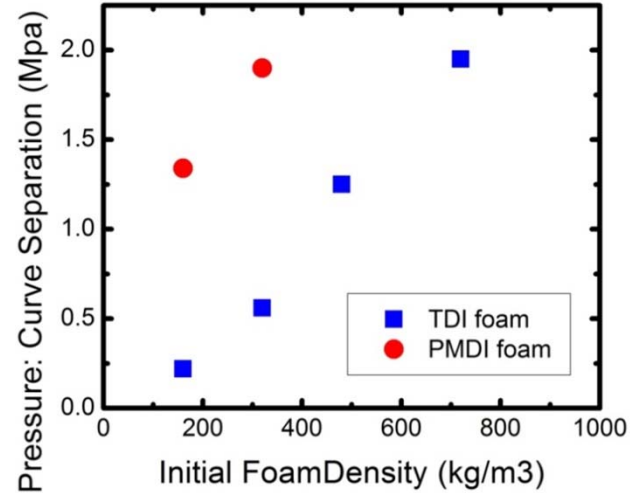
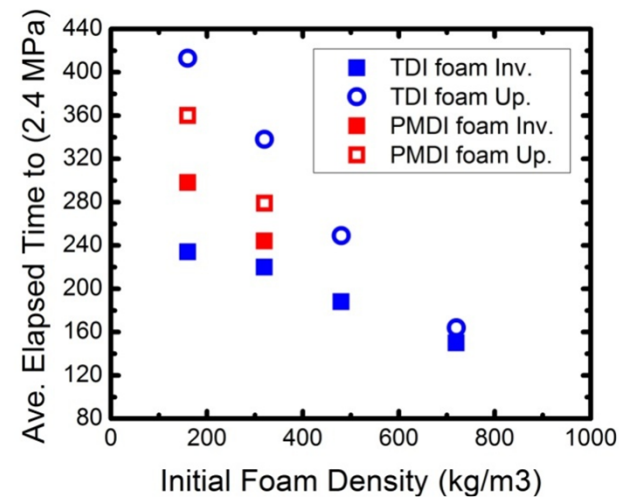
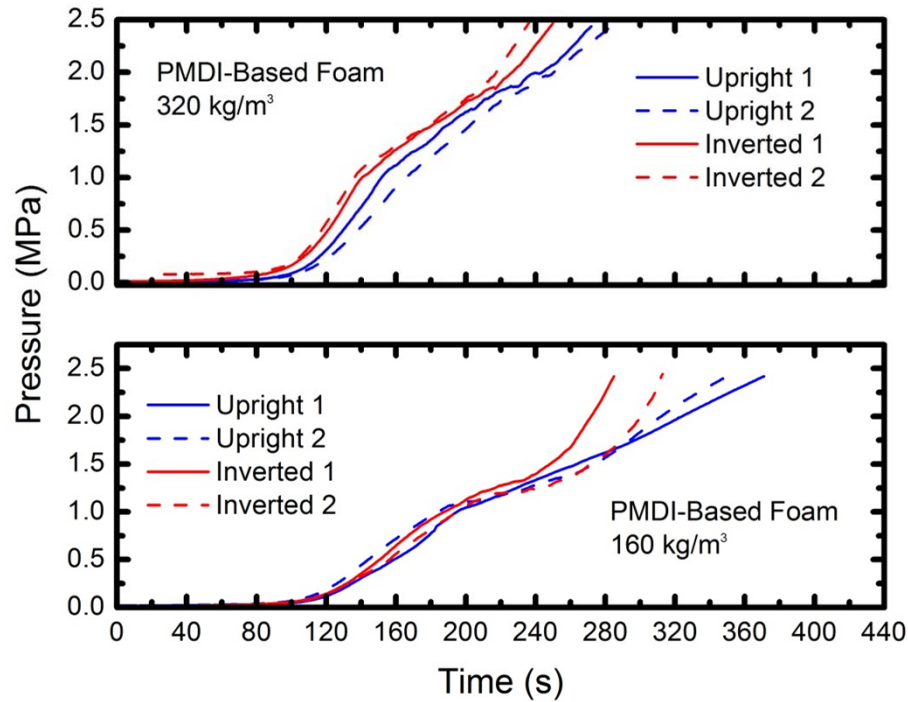
Bulk movement was toward the  heat source



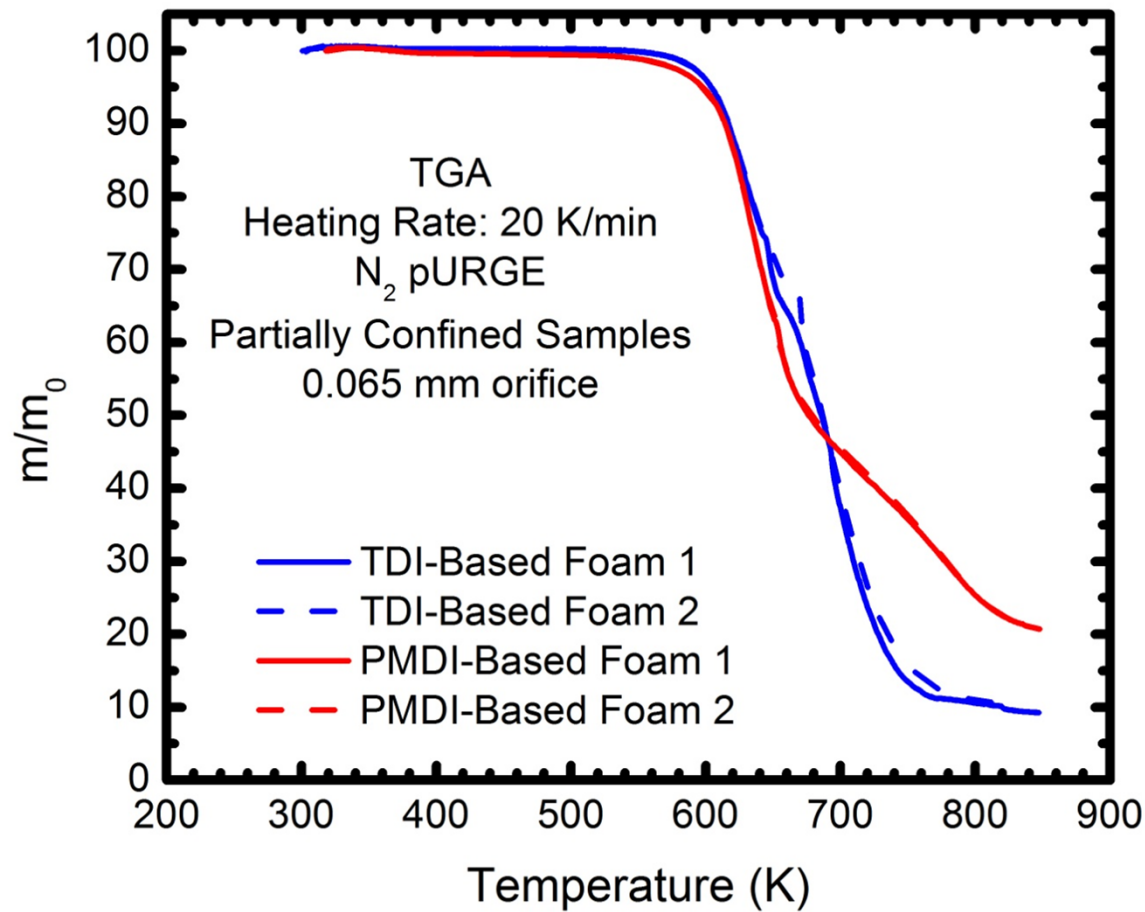
For both RPU foams, time to vent pressure (2.4 MPa) decreased as bulk density of initial foam increased



Pressures observed with PMDI-based foam samples varied less between upright and inverted samples



TDI-based foam and PMDI-based foam behave differently during thermal decomposition



Postmortem examination of samples also indicates different physical behavior (density = 160 kg/m³)



TDI-Based

Upright



PMDI-based



Inverted

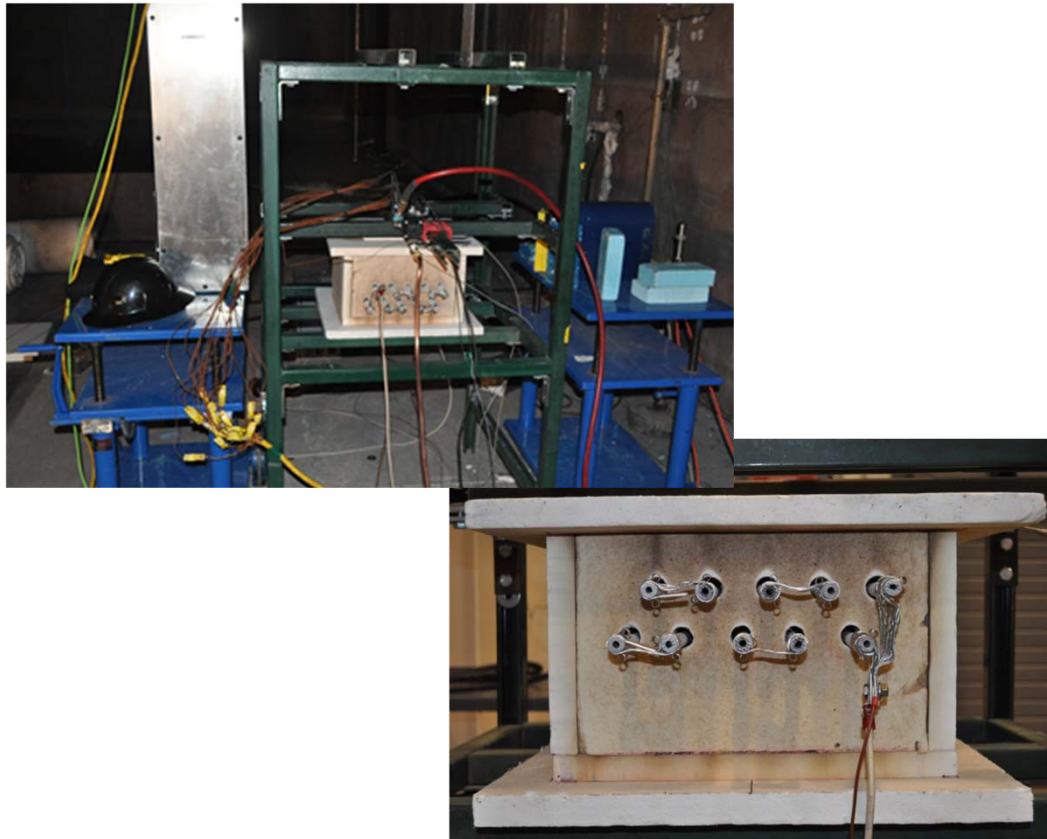




Summary of Experiments

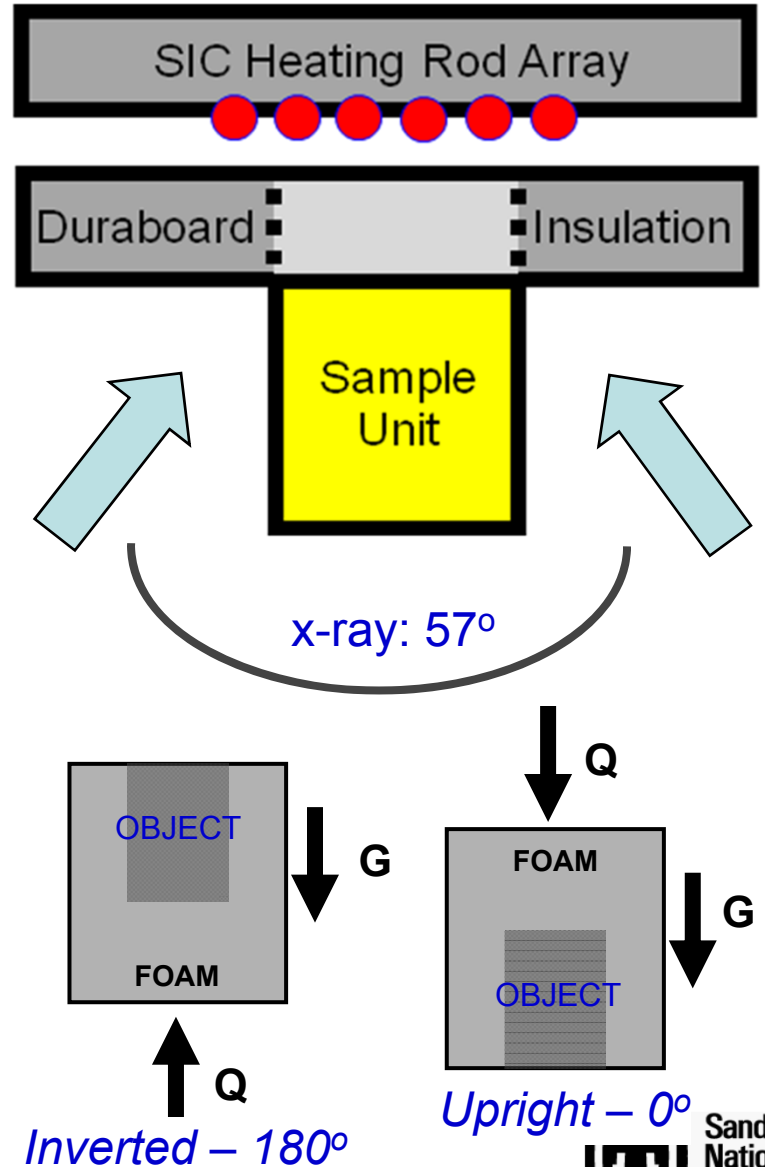
- **TDI**
 - FY2009: 224 kg/m³
 - FY2010: 160, 320, 480, 720 kg/m³
 - FY2011: 640 kg/m³ (thicker can design)
- **PMDI**
 - FY2009: 320 kg/m³
 - FY2010: 160 kg/m³
 - FY2011: 265, 365 kg/m³ (thicker can design)

Thicker can design and different heat source



Sample container

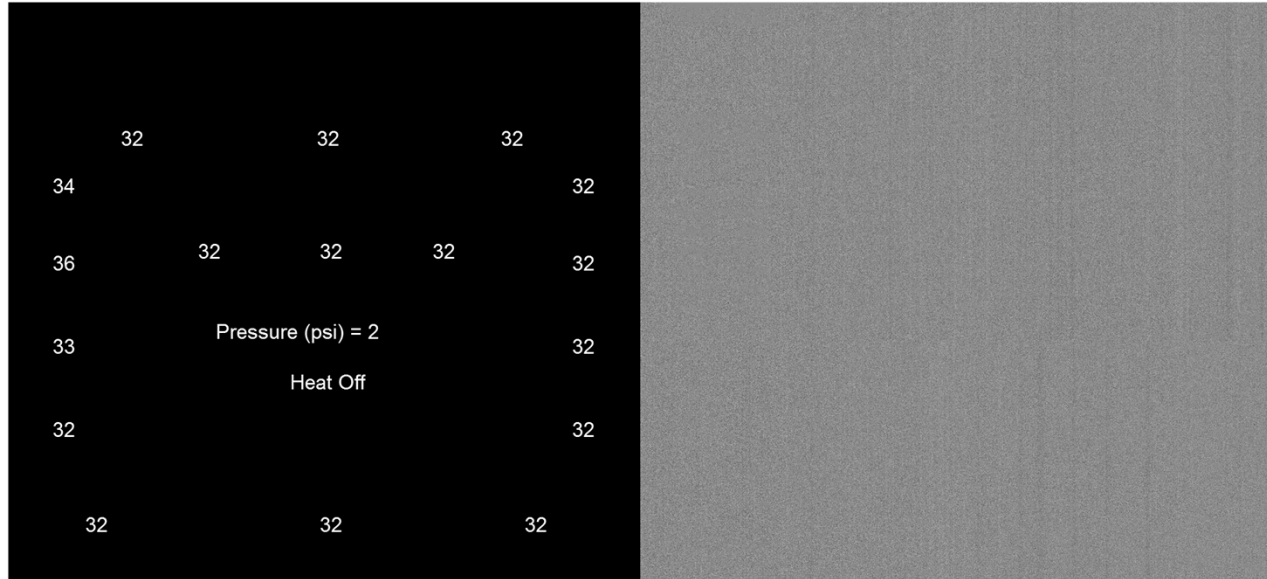
- Sleeve 321 SS tubing
 - 8.89-cm OD, 5.40 cm long
 - 1.651-mm wall thickness
- End plates: 0.602-cm thick 304 SS
 - Laser welded to Sleeve



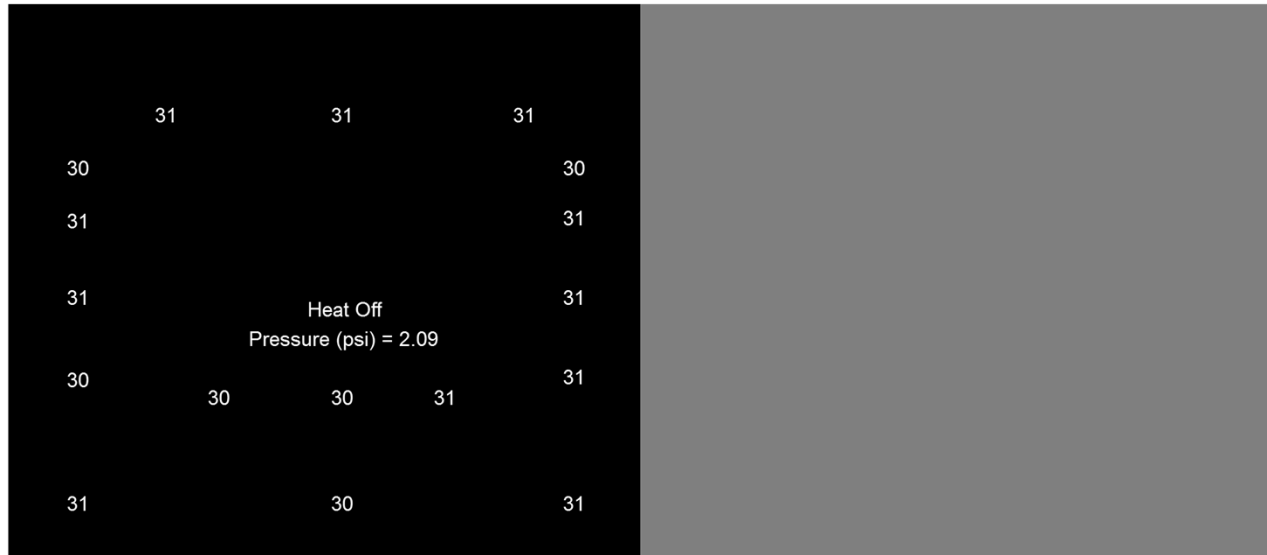
X-ray images showed liquefaction and flow occurring with lower density PMDI-based polyurethane foam

PMDI-based foam
320 kg/m³

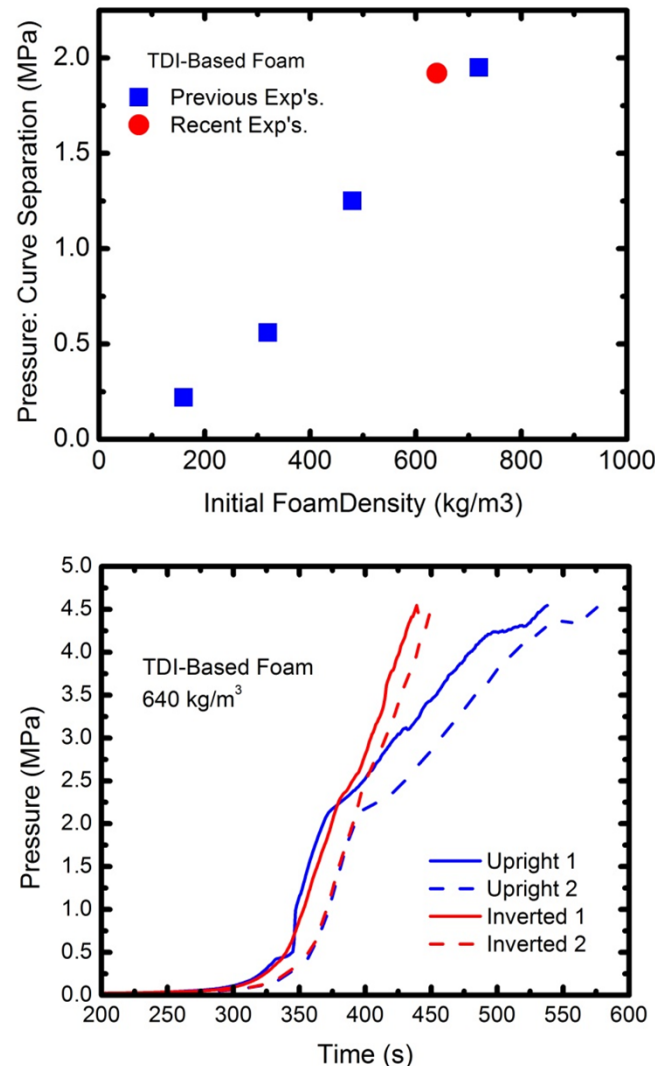
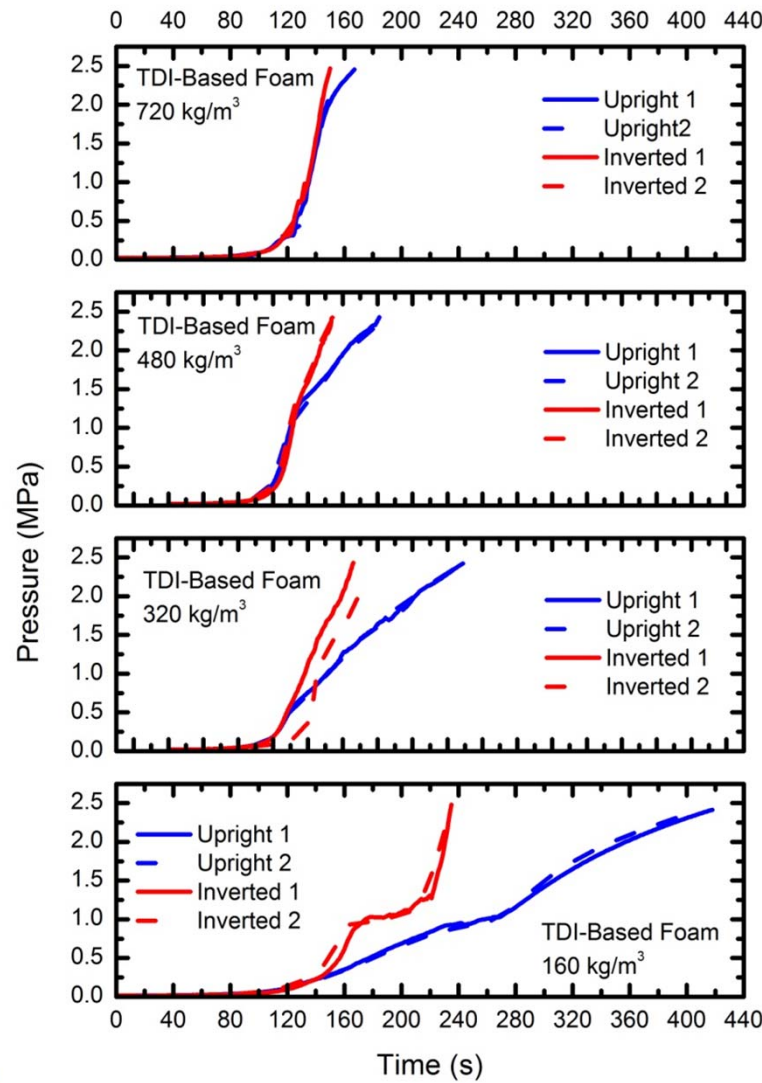
Bulk movement
was away from →
the heat source



Bulk movement
was toward the →
heat source

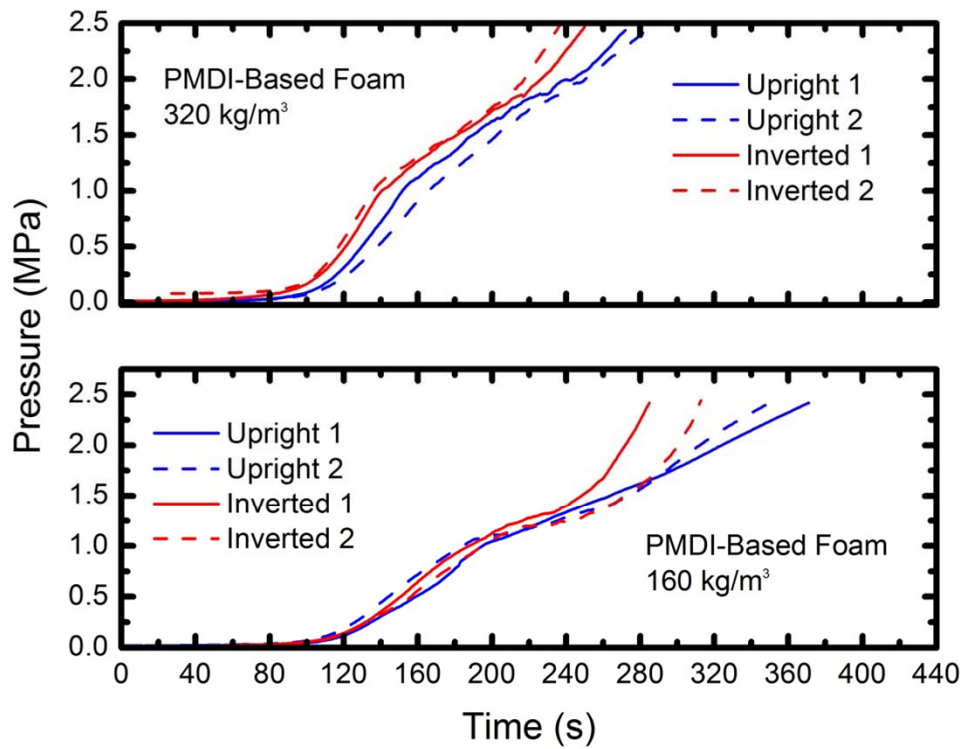


For both RPU foams, time to vent pressure (2.4 MPa) decreased as bulk density of initial foam increased

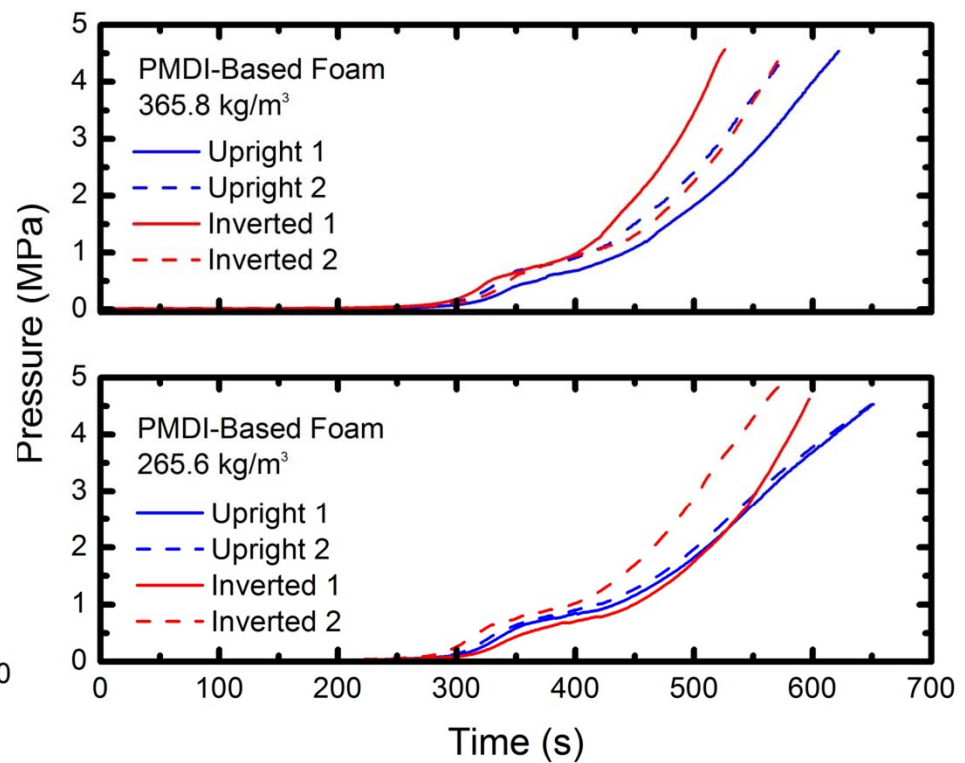


Pressures observed with PMDI-based foam samples varied less between upright and inverted samples

Thin Can/Radiant Heat Lamps



Thick Can/Silicon Rods



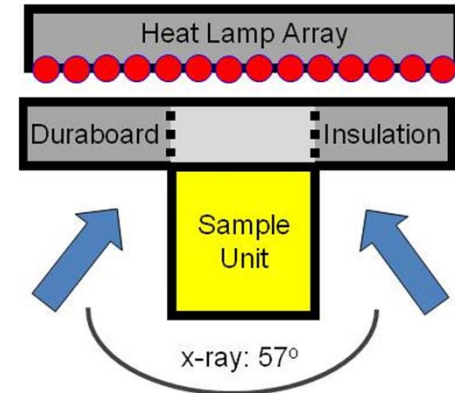
Modeling approach was based on diffusive approximation for radiant heat transfer

Energy Balance

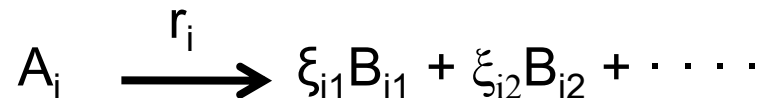
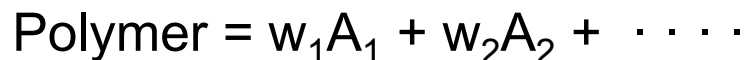
$$\rho c \frac{\partial T}{\partial t} = \nabla \bullet (k + k_e) \nabla T + \sum_i \rho r_i (-\Delta H_i)$$

Diffusive approximation:
Optically thick material

$$k_e = \frac{16\sigma}{3(a + \sigma_s)} T^3$$



Decomposition reactions / rates (r_i)



$$\frac{dw_{A_i}}{dt} = -k_i w_{A_i} = -r_i \quad \frac{d\bar{\rho}_{B_{ij}}}{dt} = \rho_B^0 \frac{\xi_{ij} w_i^0}{\bar{M}_{B_{ij}}} k_i w_{A_i}$$

$$k_i = k_i^0 \exp(-Q_i/RT)$$

Pressure - Assume

- Gradients relax quickly
- Ideal gas law
- All decomp. prod. \uparrow
- Gas occupies all free volume

$$P = \frac{n_g R}{\int_{V_g} \frac{1}{T} dV_g}$$

Values for ρ , c , k , and k_e were obtained from available literature or independent exp's.

- Density (ρ) was determined by measuring/weighing samples
- Heat capacity (c_p) values were taken from available literature and were consistent with DSC results
- Thermal conductivity (k) values were taken from available literature
- Effective radiative conductivity k_e was determined using an integrating sphere apparatus to measure reflectance and transmittance through un-reacted foam
- Scattering (σ_s) and absorption (a) coefficients were calculated using an analytical two-flux representation of radiative transfer

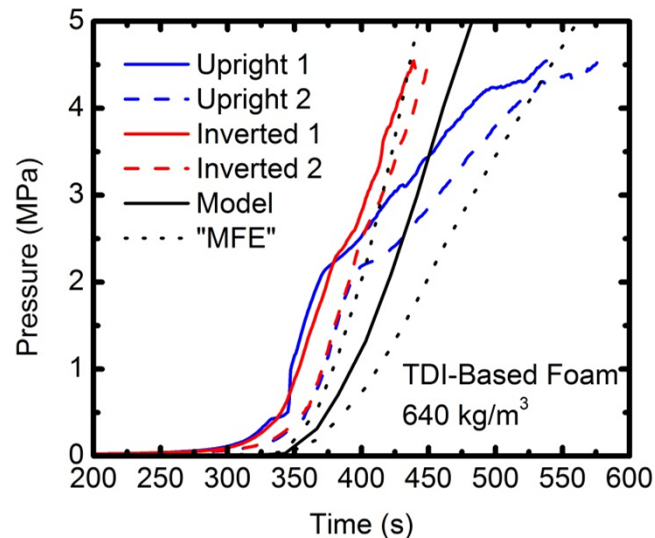
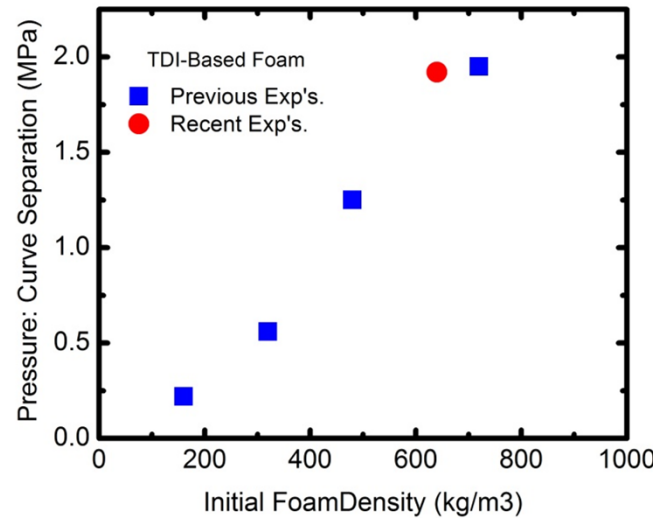
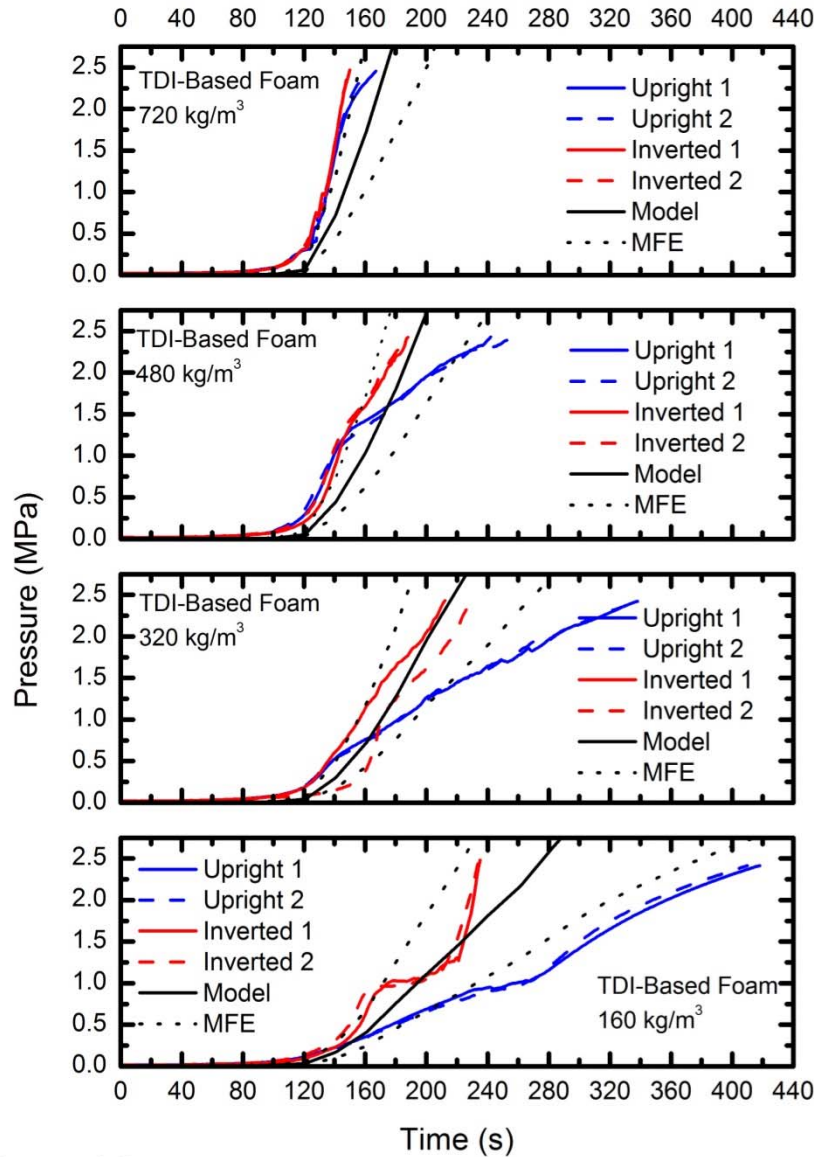
$$k_e = \frac{16\sigma}{3(a + \sigma_s)} T^3 \quad \text{or} \quad k_e = \frac{0.003\sigma}{f_{rxn}} T^3 \text{ W/mK}$$

Multiple techniques were used to examine decomposition mechanisms and obtain rate data

- Decomposition rates and evolved gas/vapor products
 - TGA-FTIR
 - Pyrolysis-GC-FTIR
- Postmortem condensed-phase analyses
 - FTIR - ATR
- Specific heat and enthalpy changes
 - DSC simultaneous DSC-TGA

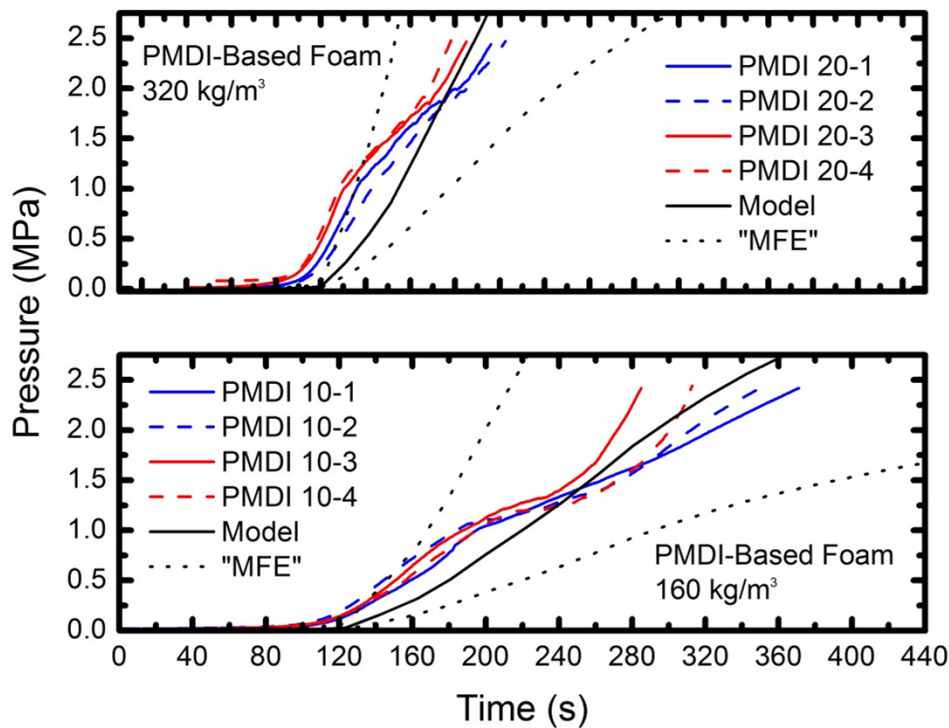
Initial Foam $w_1^0 A_1 + w_2^0 A_2 + \dots + w_n^0 A_n$	Reaction \longrightarrow	Decomposition Products
A_1	r_1	$\xi_{11} B_{11} + \xi_{12} B_{12} + \dots + \xi_{1m} B_{1m}$
A_2	r_2	
...	...	$\xi_{21} B_{21} + \xi_{22} B_{22} + \dots + \xi_{2m} B_{2m}$
A_n	r_n	$\xi_{n1} B_{n1} + \xi_{n2} B_{n2} + \dots + \xi_{nm} B_{nm}$

Model and Experimental Comparison TDI-Based Foam

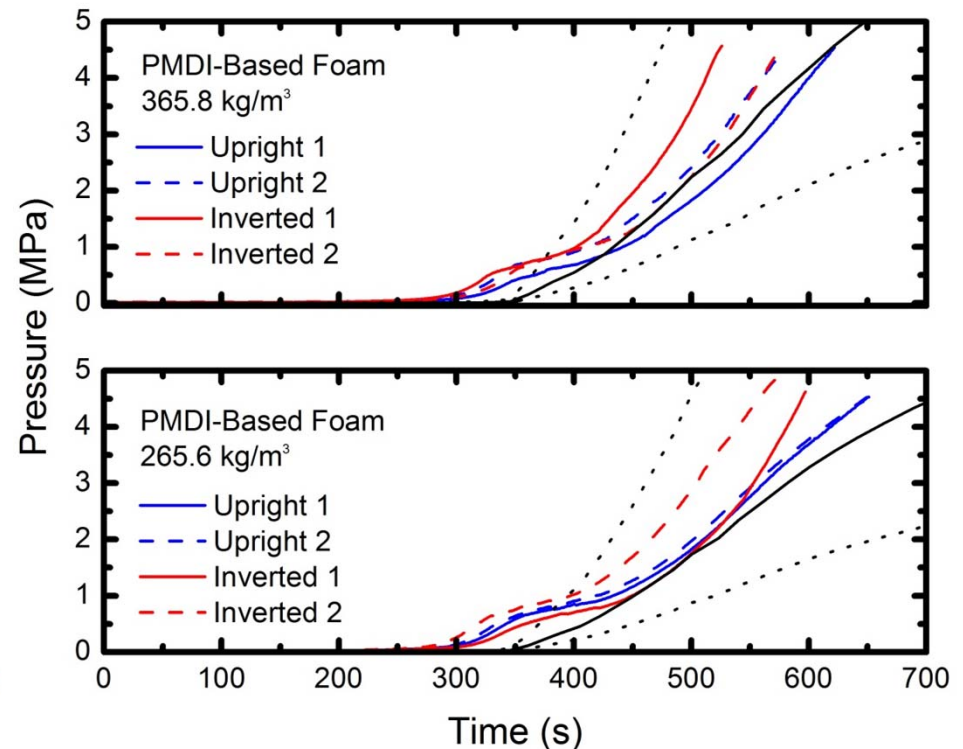


Model and Experimental Comparison PMDI-Based Foam

Thin Can/Radiant Heat Lamps



Thick Can/Silicon Rods

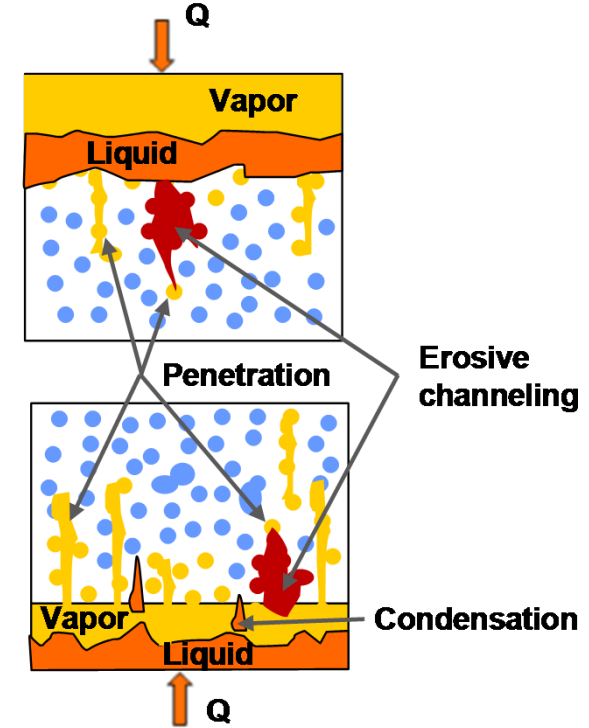


Foam density and structure determine physical behavior during thermal decomposition

- Rate of container pressurization depends on physical behavior
- Low-density (160 kg/m^3) TDI based-foam
 - Significant convective heat transfer was caused by
 - Liquefaction and flow
 - Penetration and erosive channeling by hot gases
- In pressure range previously studied (ambient to 2.4 MPa), magnitude of effects decreased as foam density increased
- In recent work (ambient to 4.5 MPa), difference between upright and inverted samples increased significantly above $\sim 2.5 \text{ Mpa}$
- Sources of Model Form Error (MFE)
 - Convective heat transfer (gas permeation in pores structure and liquefaction and flow) causes MFE in current model
 - Heat transfer to foam and, therefore, the amount of foam that has decomposed as a function of time
 - Volume that is available to the gas phase as a function of time
 - A related MFE is the distribution of organic decomposition products between condensed and vapor phases

Future work to reduce model form error and include additional physics

- **Liquefaction and flow of decomposition products**
 - *Significantly impacts heat transfer to foam/ rate of gas generation and container pressurization*
- **Gas penetration into pores and erosive channeling by hot gas-phase decomposition products**
- **Vapor-liquid distribution of organic decomposition products**
- **To support model/code development, future experiments will examine:**
 - *Rheological properties of decomposing foams*
 - *Permeability and porosity as a function of temperature*
 - *Vapor–liquid distribution of organic decomposition products*
 - *Higher pressures*





Modeling Foam Decomposition with a Porous Media Approach

A. B. Dodd, K. L. Erickson, D. J. Glaze, and R.
E. Hogan Jr.

Sandia National Laboratories
Albuquerque, New Mexico, USA

VNIIA-SNL Technical Exchange

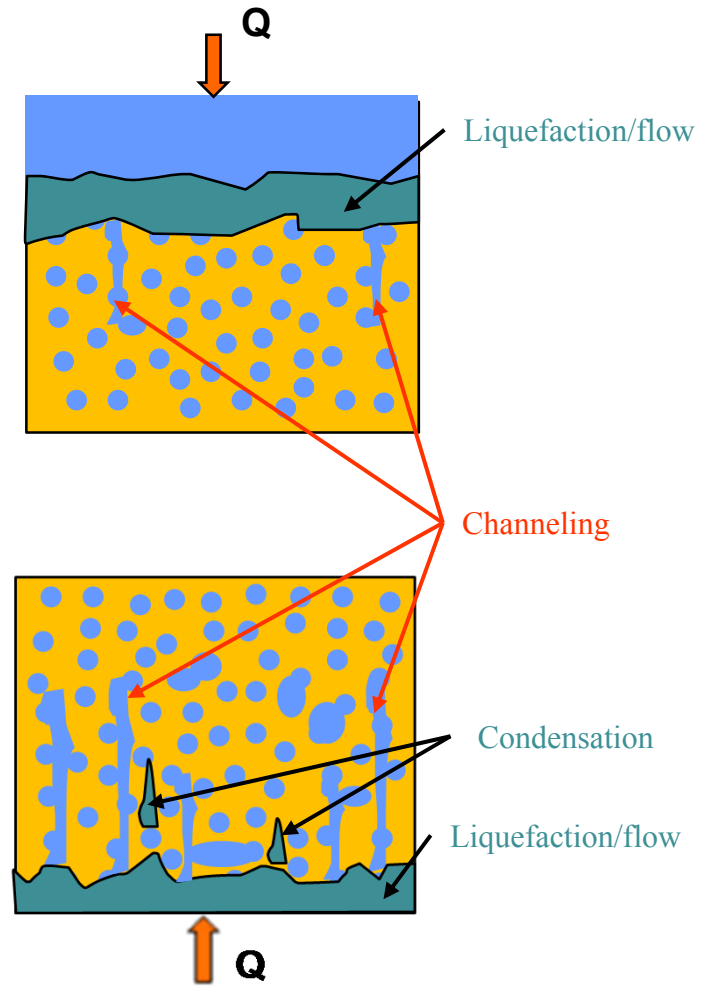
6-9 August 2012

Sandia is a multi program laboratory operated by Sandia Corporation, a Lockheed Martin Company,
for the United States Department of Energy's National Nuclear Security Administration
under contract DE-AC04-94AL85000.



Foam Decomposition Phenomenology

- Heat transfer
- Mass transfer
- Chemistry
- Liquefaction/flow of decomposition products
 - *Significantly impacts heat transfer to foam / rate of gas generation and container pressurization*
- Erosive channeling by hot gas-phase decomposition products
- Vapor-Liquid Distribution of Organic Decomposition Products



Experimental and Modeling Efforts

- **Objective: Develop a predictive modeling capability**
- **Approach: Hierarchical approach with incremental improvements to modeling and experimental capabilities**
 - Modeling:
 - Provide today's capability with enhancements as appropriate
 - Develop a plan for future capabilities to be developed incrementally with increasing complexity
 - Implement new code capability, verify, validate
 - Assess feasibility of approach
 - Modify path forward
 - Experimentally
 - Develop additional experimental capabilities
 - Perform range of scale experiments to examine phenomenology



Porous Media Capability

- **Solve conservation equations for:**
 - Mass (gas phase, condensed phase)
 - Species (gas phase, condensed phase)
 - Energy (gas phase, condensed phase)
- **Physics include:**
 - Condensed phase and gas phase conduction
 - Gas phase convection
 - Species diffusion
 - Darcy flow
 - Generalized reaction capability
- **Interface with fluid region**

Currently Implemented Equations

Mass Conservation Equations:

Condensed Phase: $\frac{\partial \bar{\rho}}{\partial t} = -\dot{\omega}_{fg}'''$

Gas Phase: $\frac{\partial(\bar{\psi}\rho_g)}{\partial t} + \frac{\partial(\rho_g u_i)}{\partial x_i} = \dot{\omega}_{fg}'''$

where: $\dot{\omega}_{fg}'''$ = Formation rate of gases from condensed phase

$$u_i = -\frac{\bar{K}}{\mu} \left(\frac{\partial P}{\partial x_i} + \rho_g g_i \right) \quad \text{(Darcy velocity with buoyancy correction)}$$

$$\rho_g = \frac{PM}{R_u T_g} \quad \text{(Ideal gas law)}$$

$$\bar{\psi} = \sum_k X_k \psi_k \quad \text{(Porosity, from volume-averaged species porosities)}$$

$$\bar{K} = \sum_k X_k K_k \quad \text{(Permeability, from volume-averaged species permeabilities)}$$

$$\psi_k = 1 - \frac{\rho_k}{\rho_{s0,k}} \quad X_k = \bar{\rho} \frac{Y_k}{\rho_k}$$

Currently Implemented Equations

Species Conservation Equations:

Condensed Phase:
$$\frac{\partial(\bar{\rho} Y_k)}{\partial t} = (\dot{\omega}_{fk}''' - \dot{\omega}_{dk}''')$$

Gas Phase:
$$\frac{\partial(\bar{\psi} \rho_g Y_k)}{\partial t} + \frac{\partial(\rho_g u_i Y_k)}{\partial x_i} = -\frac{\partial}{\partial x_j} \left(-\bar{\psi} \rho_g D \frac{\partial Y_k}{\partial x_j} \right) + (\dot{\omega}_{s,fk}''' - \dot{\omega}_{s,dk}''') + (\dot{\omega}_{g,fk}''' - \dot{\omega}_{g,dk}''')$$

where: $(\dot{\omega}_{fk}''' - \dot{\omega}_{dk}''')$ = Formation and destruction rate of condensed-phase species due to heterogeneous reactions

$(\dot{\omega}_{s,fk}''' - \dot{\omega}_{s,dk}''')$ = Formation and destruction rate of gas-phase species due to heterogeneous reactions

$(\dot{\omega}_{g,fk}''' - \dot{\omega}_{g,dk}''')$ = Formation and destruction rate of gas-phase species due to homogeneous reactions

Currently Implemented Equations

Enthalpy Conservation Equations:

Condensed Phase:
$$\frac{\partial(\bar{\rho}\bar{h})}{\partial t} = -\frac{\partial}{\partial x_j} \left(\bar{k} \frac{\partial \bar{T}}{\partial x_j} \right) + \sum_k (\dot{\omega}_{fk}''' - \dot{\omega}_{dk}''') h_k - h_{cv} (\bar{T} - T_g)$$

Gas Phase:
$$\frac{\partial(\bar{\psi} \rho_g h_g)}{\partial t} + \frac{\partial(\rho_g u_i h_g)}{\partial x_i} = -\frac{\partial}{\partial x_j} \left(-\bar{\psi} \rho_g D \frac{\partial h_g}{\partial x_j} \right) + \left(\bar{\psi} \frac{\partial P}{\partial t} + u_j \frac{\partial P}{\partial x_j} \right) + \sum_k (\dot{\omega}_{s,fk}''' - \dot{\omega}_{s,dk}''') h_{g,k} + h_{cv} (\bar{T} - T_g)$$

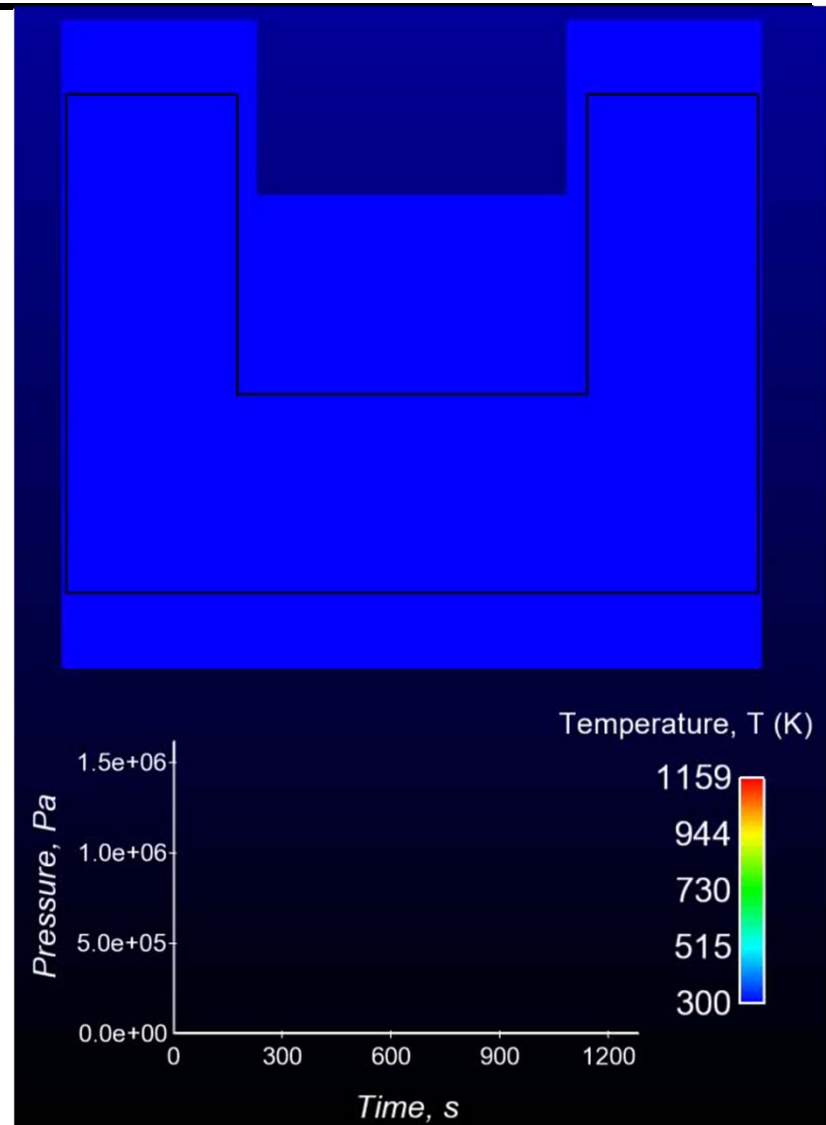
where: h_{cv} = Volumetric heat transfer coefficient

$$\bar{k} = \sum_k X_k k_k \quad (\text{Volume-averaged conductivity})$$

$$\bar{h} = \sum_k Y_k h_k \quad (\text{Mass-averaged enthalpy})$$

Coupling of Porous Media and Conduction Region

- **Loosely-coupled solution strategy:**
 - Solve conduction region
 - Transfer interface T to porous region as a Dirichlet BC
 - Solve porous region
 - Transfer interface heat flux to conduction region as a flux BC
- **Pressurizing foam-in-a-can simulations now possible**





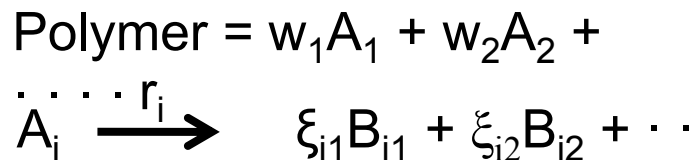
Modeling Path Forward

- **Porous media approach coupled with fluid region**
 - Two phase: gas/solid
 - Three phase: gas/liquid/solid
 - Material expansion
- **Front tracking methods**
 - Decomposition front with gas domain formation
 - Liquefaction and flow
- **Vapor/Liquid Equilibrium (approximations?)**
- **Participating media radiation**



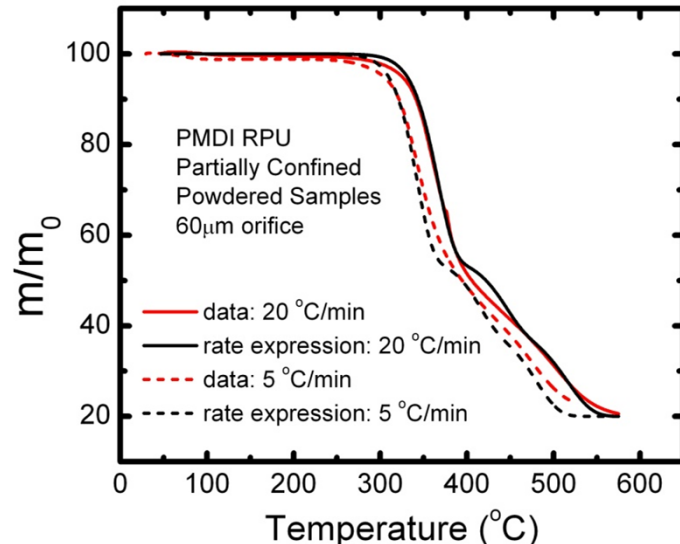
Backup Slides

TGA-FTIR and DSC provided data for rate expressions, evolved gases, and ΔH



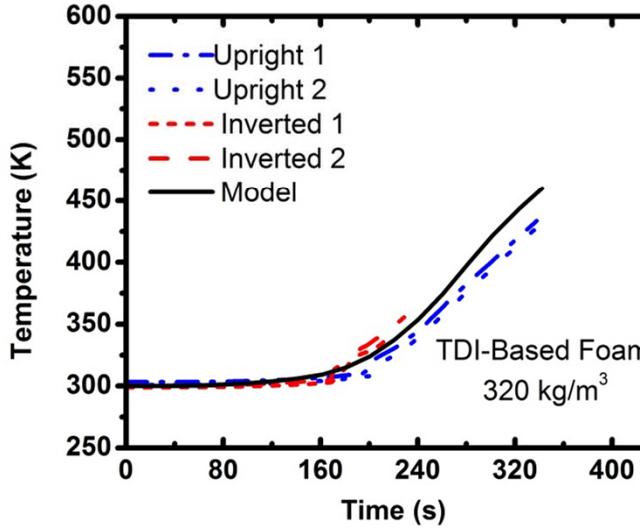
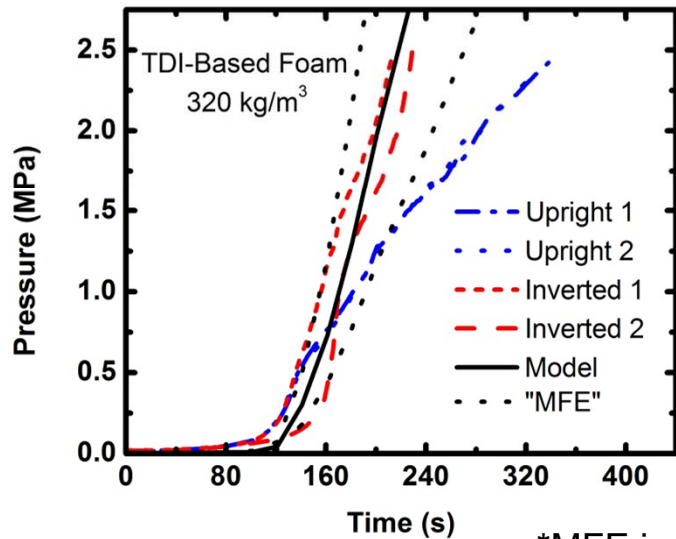
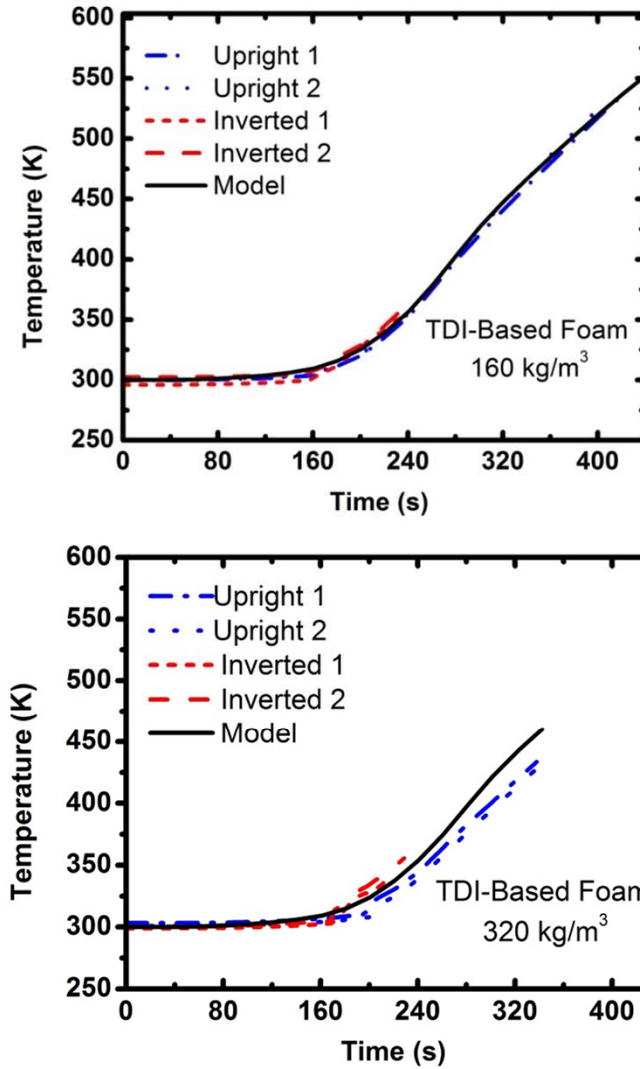
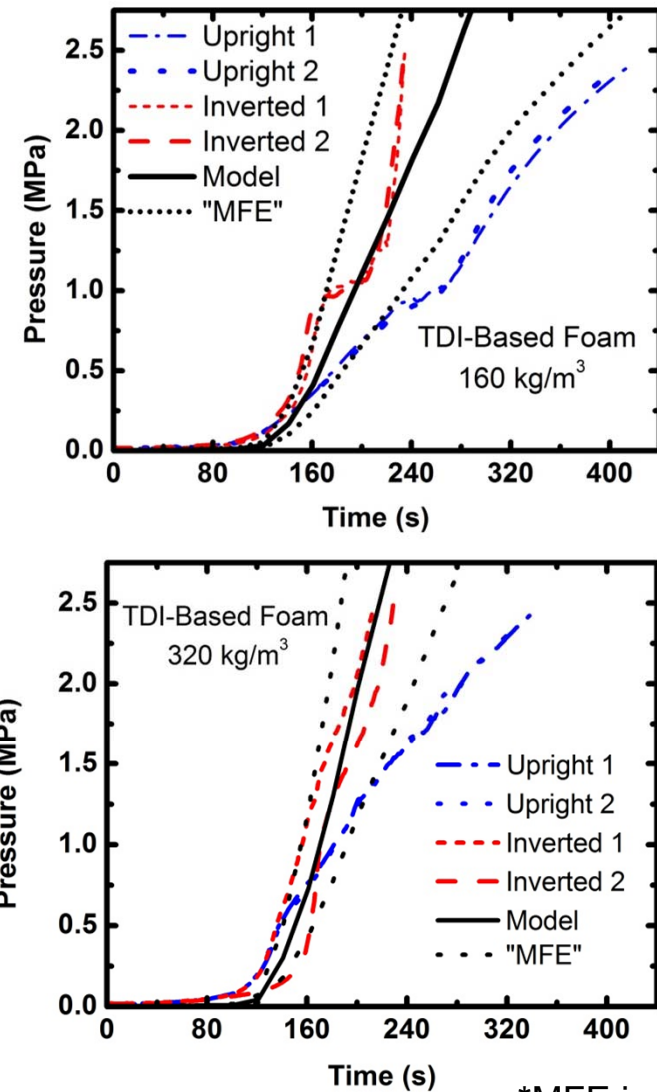
$$\frac{dw_{A_i}}{dt} = -k_i w_{A_i} = -r_i \quad \frac{d\bar{\rho}_{B_{ij}}}{dt} = \rho_B^0 \frac{\xi_{ij} w_i^0}{\bar{M}_{B_{ij}}} k_i w_{A_i}$$

$$k_i = k_i^0 \exp(-Q_i/RT)$$



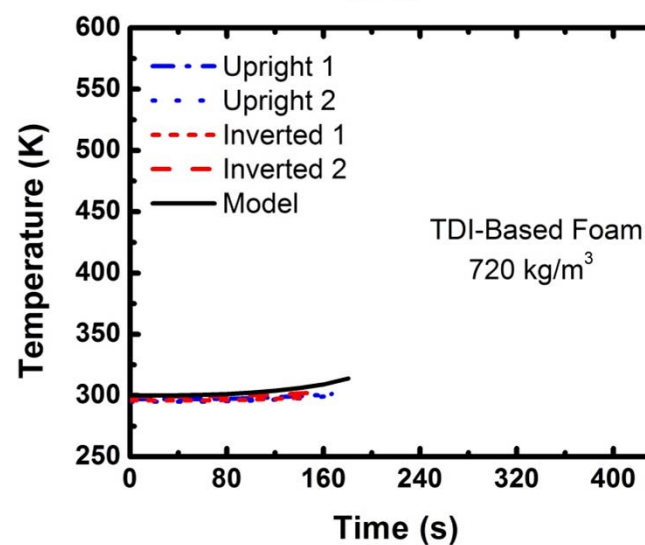
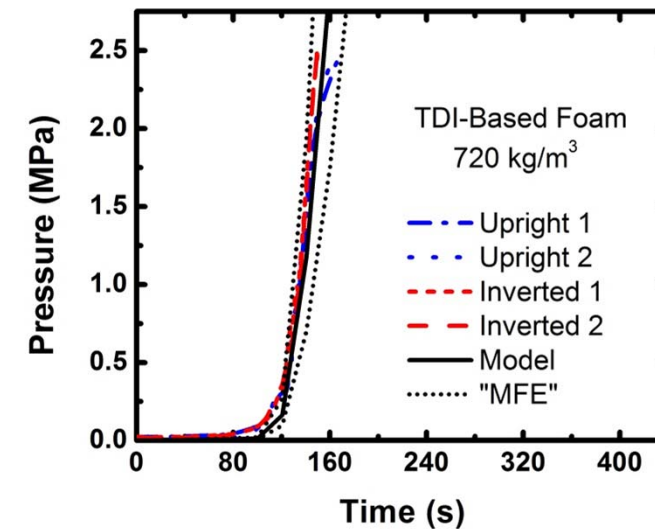
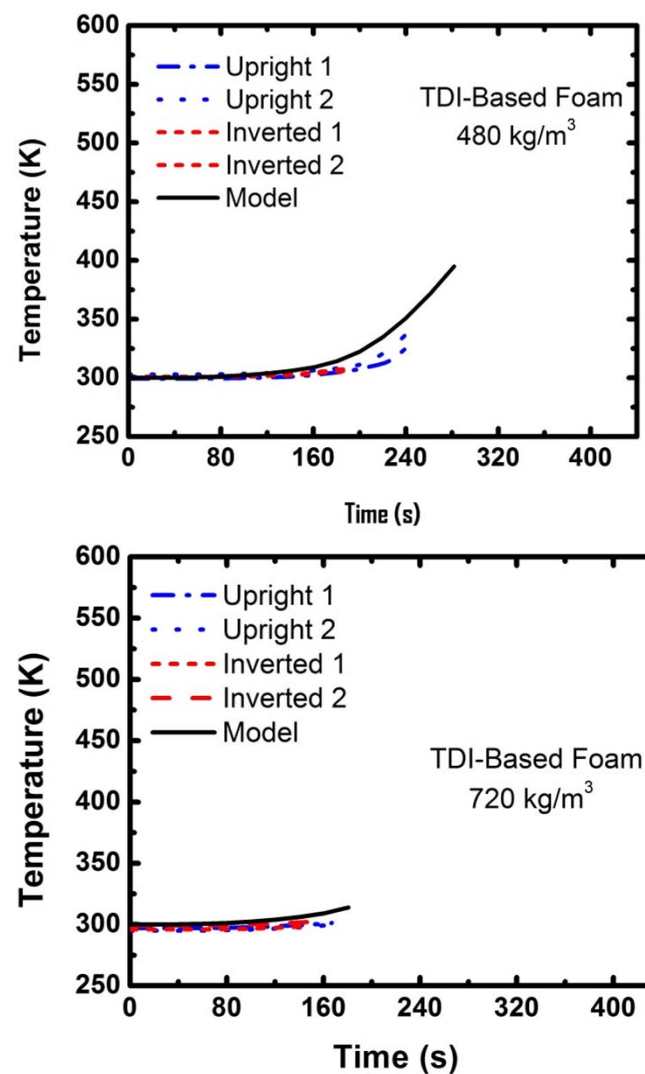
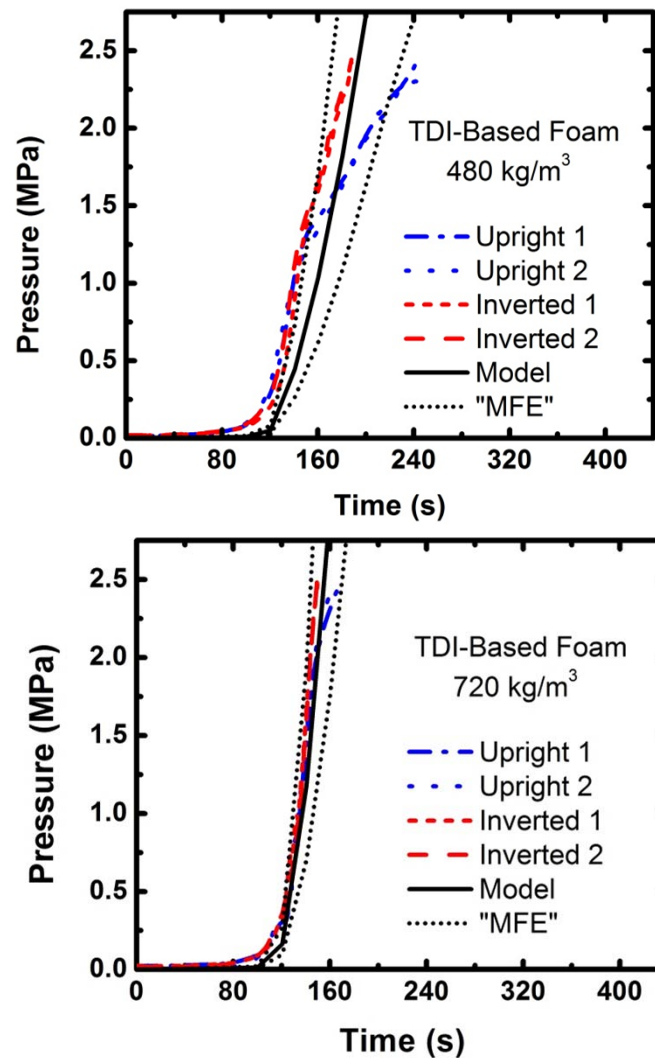
A_i	W_i	ξ_{ij}	Decomposition Products	MW (kg/mole)	ΔH kJ/kg	K^0 (s ⁻¹)	Q/R (K)
A_1	0.45	0.56	CO ₂	44	0	8.0x10 ¹²	21,600
		0.44	Organic vapors	~80			
A_2	0.15	1.0	Organic Vapors	~120	0	1.8x10 ¹¹	21,600
A_3	0.40	0.50	Organic Vapors	~120	0	8.9x10 ⁹	21,600
		0.50	Char				

Current simulations do not account for convective heat transfer by gases or liquids

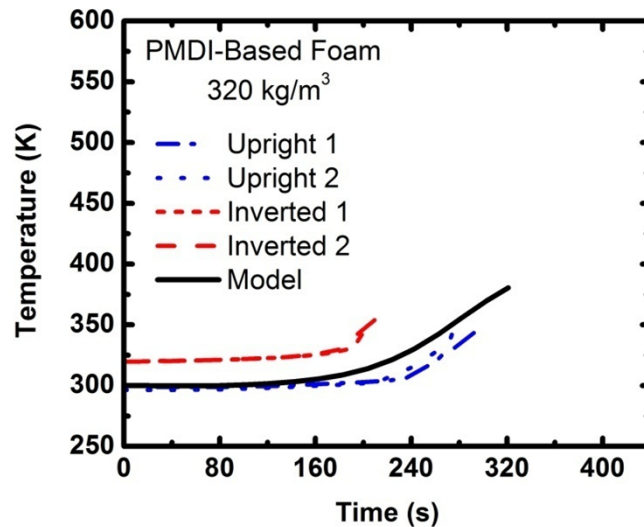
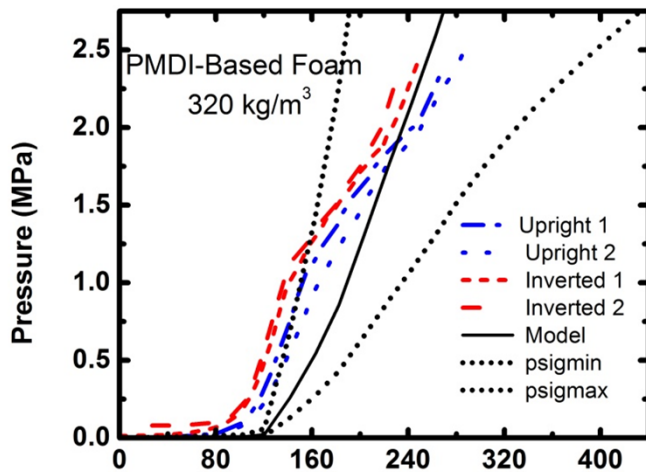
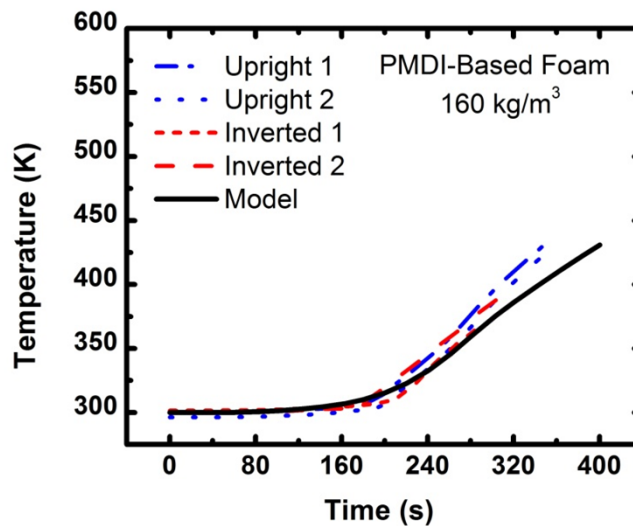
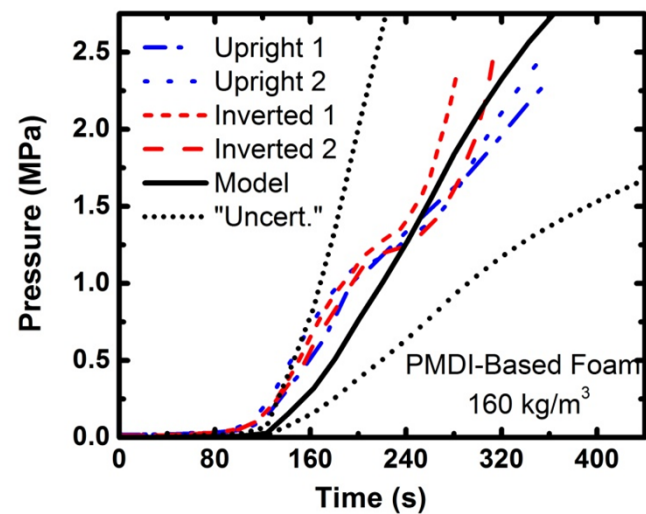


*MFE is Model Form Error

Difference between experimental and modeling results is less with higher density TDI-based foams



Similar results were obtained for PMDI-based foams



Mass and Species Porous Media Equations

Condensed Phase

Mass Conservation

$$\frac{\partial \bar{\rho}}{\partial t} = -\dot{\omega}_{fg}'''$$

Species Conservation

$$\frac{\partial (\bar{\rho} Y_i)}{\partial t} = \dot{\omega}_{fi}''' - \dot{\omega}_{di}'''$$

Gas Phase

Mass Conservation

$$\frac{\partial (\bar{\psi} \rho_g)}{\partial t} = \nabla \cdot \left(\frac{\rho_g \bar{K}}{\mu_g} (\nabla P + \rho_g \vec{g}) \right) + \dot{\omega}_{fg}'''$$

Species Conservation

$$\frac{\partial (\bar{\psi} \rho_g Y_j)}{\partial t} = \nabla \cdot \left(\frac{\rho_g Y_j \bar{K}}{\mu_g} (\nabla P + \rho_g \vec{g}) \right) + \nabla \cdot (\bar{\psi} \rho_g D \nabla Y_j) + \dot{\omega}_{s,fj}''' - \dot{\omega}_{s,dj}''' + \dot{\omega}_{g,fj}''' - \dot{\omega}_{g,dj}'''$$



Condensed and Gas Phase Energy and Momentum Equations

Energy Conservation Condensed Phase

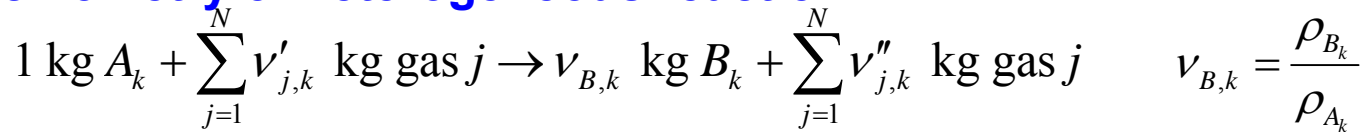
$$\frac{\partial(\bar{\rho}\bar{h})}{\partial t} = \nabla \cdot \bar{k} \nabla T + \sum_{k=1}^K \dot{Q}_{s,k}''' + \sum_{i=1}^M (\dot{\omega}_{fi}''' - \dot{\omega}_{di}''') h_i - h_{cv} (T - T_g)$$

Energy Conservation Gas

Phase
$$\frac{\partial(\bar{\psi}\rho_g\bar{h}_g)}{\partial t} = \nabla \cdot \left(\frac{\rho_g\bar{h}_g\bar{K}}{\mu_g} (\nabla P + \rho_g \vec{g}) \right) + \nabla \cdot (\bar{\psi}\rho_g D \nabla \bar{h}_g) + \sum_{\ell=1}^L \dot{Q}_{g,\ell}''' + \sum_{j=1}^N (\dot{\omega}_{s,fj}''' - \dot{\omega}_{s,dj}''') h_{g,j}^* + h_{cv} (T - T_g)$$

Heterogeneous Reactions

Stoichiometry of heterogeneous reaction k



Destruction rate of condensed-phase species A_k

$$\dot{\omega}_{dA_k}''' = \left(\frac{\bar{\rho} Y_{A_k}}{\left(\bar{\rho} Y_{A_k} \right)_{\Sigma}} \right)^{n_k} \left(\bar{\rho} Y_{A_k} \right)_{\Sigma} Z_k \exp\left(-\frac{E_k}{RT}\right) \quad (\text{for } n_{O_2,k} = 0)$$

$$\dot{\omega}_{dA_k}''' = \left(\frac{\bar{\rho} Y_{A_k}}{\left(\bar{\rho} Y_{A_k} \right)_{\Sigma}} \right)^{n_k} \left(\bar{\rho} Y_{A_k} \right)_{\Sigma} \left[\left(1 + Y_{O_2} \right)^{n_{O_2,k}} - 1 \right] Z_k \exp\left(-\frac{E_k}{RT}\right) \quad (\text{for } n_{O_2,k} \neq 0)$$

Formation rate of condensed-phase species B_k

$$\dot{\omega}_{fB_k}''' = \nu_{B,k} \dot{\omega}_{dA_k}''' = \frac{\rho_{B_k}}{\rho_{A_k}} \dot{\omega}_{dA_k}'''$$

$$\dot{\omega}_{fg_k}''' = \left(1 - \nu_{B,k} \right) \dot{\omega}_{dA_k}''' = \left(1 - \frac{\rho_{B_k}}{\rho_{A_k}} \right) \dot{\omega}_{dA_k}'''$$

Conversion rate of condensed-phase mass to gas-phase mass

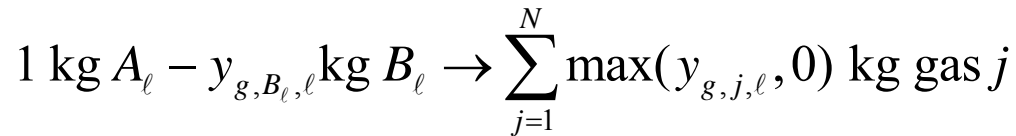
Net formation rate and destruction rate of gaseous species j from reaction k

$$\dot{\omega}_{s,fj,k}''' = \dot{\omega}_{fg_k}''' y_{s,j,k} \quad \dot{\omega}_{s,dj,k}''' = -\dot{\omega}_{fg_k}''' y_{s,j,k}$$

$$\dot{Q}_{s,k}''' = -\dot{\omega}_{dA_k}''' \Delta H_k$$

Homogeneous Reactions

Stoichiometry of homogeneous reaction ℓ



Destruction rate of gas-phase species A_ℓ

$$\dot{\omega}_{dA_\ell}''' = \bar{\psi} [A_\ell]^{p_\ell} [B_\ell]^{q_\ell} T^{b_\ell} Z_\ell \exp\left(-\frac{E_\ell}{RT_g}\right)$$

Net formation rate and destruction rate of gaseous species j by homogeneous gaseous reaction $\dot{\omega}_{g,fj,\ell}''' = \dot{\omega}_{dA_\ell}''' y_{g,j,\ell}$

$$\dot{\omega}_{g,dj,\ell}''' = -\dot{\omega}_{dA_\ell}''' y_{g,j,\ell}$$

Heat of reaction:

$$\dot{Q}_{g,\ell}''' = -\dot{\omega}_{dA_\ell}''' \Delta H_\ell$$

